Maintenance of transient chaos using a neural-network-assisted feedback control

J. F. Louvier-Hernández and R. Rico-Martínez
Departamento de Ingeniería Química, Instituto Tecnológico de Celaya, Avenida. Tecnológico y A. García Cubas s/n, 38010, Celaya, Guanajuato, Mexico

P. Parmananda
Facultad de Ciencias, UAEM, Avenida Universidad 1001, Col. Chamilpa, Cuernavaca, Morelos, Mexico
(Received 15 July 2001; published 13 December 2001)

A stable period-3 orbit in the parametric vicinity of a chaotic attractor is destabilized using two distinct feedback strategies. This results in the inception and subsequent maintenance of the otherwise short-lived chaotic transients. Both the techniques employed are based on the exclusion of trajectories from the near vicinity of the open loop stable period-3 attractor; the first relies on the traditional proportional feedback method while the second one includes a predictive term enabling delimitation of exclusion zones for the system dynamics. The implementation of these strategies involves construction of appropriate reference models in the form of an artificial-neural-network approximator.

DOI: 10.1103/PhysRevE.65.016203 PACS number(s): 05.45.Ac, 05.45.Gg, 82.40.Bj, 87.18.Sn

I. INTRODUCTION

It was generally believed that chaotic behavior is detrimental to the system performance. It may produce undesirable vibrations, irregular operation, and fatigue in mechanical systems. It could risk secure operation of chemical systems due to uncontrolled temperature variations. The paper on chaos control by Ott *et al.* [1] was, therefore, received with immense enthusiasm by the scientific community. The Ott-Grebogi-Yorke technique and its various variations were subsequently utilized to tame chaotic dynamics in numerous experimental situations [2–6].

It was soon realized that some systems require chaos/complexity for optimum functioning. For example, it is suggested that pathological destruction of chaotic dynamics may be implicated in certain types of brain seizures [7] and heart failures [8]. Moreover, complexity is indeed advantageous in fluid mixing [9] and heat and mass transfer in some chemical and biochemical applications. These considerations motivated the work of Yang *et al.* [10] where they achieve chaos anticontrol (preserving chaos) in a discreet map system. This concept was experimentally verified in the magnetoelastic ribbon system [11]. Subsequent to these reports, work involving maintenance of chaos has been more or less dormant.

In this paper we revisit the problem of chaos anticontrol by implementing the strategy to a numerical model simulating electrochemical corrosion [12,13]. An artificial-neural-network (ANN) reference model is constructed to predict the location of the stable periodic orbit (period 3). This enables one to tune the feedback applied and consequently stabilize the systems dynamics on chaotic transients that are otherwise short lived. The paper is organized as follows. In the following section, we discuss briefly the model system and the two control algorithms used. In Sec. III, the ANN predictor is described and representative results are presented. Finally, we offer a brief conclusion regarding the obtained results.

II. MODEL SYSTEM AND CONTROL STRATEGIES

A. Numerical model

We apply chaos anticontrol to a model for aqueous electrochemical corrosion [12,13] described by three dimensionless differential equations:

$$\dot{Y} = p(1-\theta_{OH}-\theta_O) - qY, \tag{1}$$

$$\dot{\theta}_{OH} = Y(1-\theta_{OH}-\theta_O) - [\exp(-\beta\theta_{OH}) + r]\theta_{OH} + 2s\theta_O(1-\theta_{OH}-\theta_O), \tag{2}$$

$$\dot{\theta}_O = r\theta_{OH} - s\theta_O(1-\theta_{OH}-\theta_O). \tag{3}$$

The variables θ_O and θ_{OH} represent the fraction of the electrode surface covered by two different chemical species, while Y represents the concentration of metal ions in the electrolytic solution. The parameters p, q, r, s, and β are determined by chemical reaction rates in the model. Previous numerical studies [13] have shown that this model exhibits period-3 dynamics for parameter set $\{p, q, r, s, \beta\}$ at $\{2.0\times10^{-4},\ 1.0\times10^{-3},\ 2.0\times10^{-5},\ 9.8\times10^{-5},\ 5.0\}$ and deterministic chaos in the parametric vicinity. We numerically integrate these equations using a Runge-Kutta algorithm. In the actual potentiostatic electrochemical experiments s could be related to the experimentally accessible anodic potential. The set-point (s_0) is in the period-3 window of the bifurcation diagram (computed for s) where short-lived chaotic transients are observed due to the parametric proximity to chaotic behavior. To make the simulations realistic, control strategies will be tuned based upon a reference model constructed using a time series generated by the model and fed to a neural-network approximator, much in the same way as one would apply this strategy to a real experiment. Consequently, the ANN approximator takes the form of a next-maximum map (NMM). That is, we seek a reduced representation of the dynamics that will allow us to

predict the maximum amplitude of the oscillations based upon a previous maximum for a given parameter setting. The map we seek is of the form

$$\theta_{OH_{max\,k+1}} = f(\theta_{OH_{max\,k}}; s), \tag{4}$$

where $\theta_{OH_{max\,k}}$ and $\theta_{OH_{max\,k+1}}$ are two successive maxima of the fraction of the electrode covered by the metal hydroxide film (related to the observable anodic current in real experiments) and s is the accessible control/bifurcation parameter.

B. Control algorithms

Since the control feedback is occasional, the ''enhancement'' of the chaotic behavior is achieved without changing the underlying dynamics of the system. Initially a perturbation is employed to ''pull out'' the system from the period-3 attractor subsequent to which the parameter is returned to its original setting. The dynamics of the system are then allowed to evolve until they approach the naturally stable period-3 orbit, thereby requiring another perturbation spike to maintain the chaotic transients. We implemented chaos anticontrol using two different strategies: (a) a ''simple'' proportional feedback control and, (b) a feedback-feedforward control. Both schemes involve ''occasional'' manipulation of the accessible control parameter s.

1. Proportional feedback control

Using the reduced NMM model [Eq. (4)] as the basis, a control policy involving location (prediction) of the period-3 orbit in the NMM map is implemented. The location of this attractor is used to define a small region of radius r_c surrounding one of the three points that compose the attractor. This region will be demarcated as the *control region*.

The feedback control involves perturbing the parameter s every time the coordinates of two consecutive maxima of the dynamical system form a point that lies within the *control region*. This perturbation will be proportional to the difference between the radius of the *control region* and the distance of the current point to the attractor point. In this manner, we seek to ''destabilize'' the period-3 attractor, by preventing the system from reaching it. This proportional feedback maintains the system dynamics on the chaotic transients. The control action is implemented according to the following equation:

$$s = s_0 + \alpha(r_c^2 - d^2), \tag{5}$$

where s is the manipulated parameter, s_0 is the nominal value (set point) of the parameter, r_c is the radius of the *control region*, d is the distance from the current point to the selected central point of the *control region* (one of the points of the period-3 attractor in the NMM reduced model), and α is the proportional gain of the feedback control. This point is selected arbitrarily from the three points that constitute the attractor. The location of this point is

$$(\theta_{OH_{max\,k,\,at}}, \theta_{OH_{max\,k+1,at}});$$

thus, d is obtained using the Euclidean definition of the distance as

$$d = [(\theta_{OH_{max\,k}} - \theta_{OH_{max\,k\,at}})^2 + (\theta_{OH_{max\,k+1}} - \theta_{OH_{max\,k+1\,at}})^2]^{1/2}. \tag{6}$$

Depending on the difference between d and r_c, one can have the following situations.

(1) If the current point coincides with the perimeter of the *control region* ($r_c = d$), or lies outside the *control region*, there is no control action,

$$s = s_0 + \alpha(r_c^2 - r_c^2) = s_0.$$

Therefore the parameter value does not change

(2) If the current point lies within the *control region*, i.e., $0 < d < r_c$, then the control action depends on the magnitude of d. The closer the current point is to the center of the *control region* (the point of the period-3 attractor) the stronger is the perturbation to the parameter.

(3) If the current point lies exactly on the period-3 attractor point used to define the *control region* (i.e., in the center of such region), then $d = 0$ and the maximum possible change in the parameter is applied,

$$s = s_0 + \alpha(r_c^2) = s_0 + \Delta\ \ s_{max}.$$

The maximum allowed change in the parameter, $\Delta\, s_{max}$, can be set based upon the behavior around the period-3 attractor and the value of s_0. Although, this maximum change does not have any intrinsic restriction, one should set it to move the system towards the desired chaotic dynamics. The algorithm is devised such that the parameter always returns to the reference value s_0 when the system is forced outside the *control region*. The perturbation is applied only for a short time span and hence the system mostly executes its natural dynamics.

2. Feedback-feedforward control

This control strategy uses the ANN model of the system to predict if the trajectory will enter the *control region* (as defined earlier) in the near future. Therefore, this strategy allows for a better exclusion of the trajectories from the *control region*.

At each iteration (i.e., at every maximum of the trajectory) the ANN predicts the behavior of the system for the next *three* maxima. If the third predicted maximum enters the *control region*, the control applies a corrective action anticipating such an occurrence; in addition, if the present point lies within the *control region*, then a more severe action is applied,

$$s = s_0 + \alpha(r_c^2 - d_1^2) + \gamma(r_c^2 - d_2^2). \tag{7}$$

Now d_1 is the distance from the current point to the center of the *control region*, d_2 is the same distance but from the predicted third maximum to the center of the *control region* and, γ is the proportional gain for the feedforward part of the control.

If the current and predicted points lie outside the *control region*, then no control action is applied and the parameter value is set to its nominal value s_0. If the control is active, one may have several cases.

The predicted value falls within the *control region*, but the current value is outside the *control region*, $s=s_0+\gamma(r_c^2-d_2^2)$.

The predicted falls outside the *control region*, but the current value lies inside the *control region*; $s=s_0+\alpha(r_c^2-d_1^2)$.

Both the predicted and current value lie inside the *control region*. Then one applies the full control action [Eq. (7)].

For both control strategies, we included an estimation of the error by the ANN model in predicting the location of the period-3 attractor (Fig. 2). This error is larger for the values of s near the right of the parameter window where such behavior is observed. With the data plotted in this figure, we obtained, via linear interpolation, the error in the location of the predicted period-3 attractor. Subsequently we incorporated this estimate as a correction in the predictions of the ANN that is employed to calculate the control actions. This enhances the performance of both controllers.

III. RESULTS AND DISCUSSION

First we address the predictive capabilities of the ANN model constructed, as well as its training. After this description, we present the results obtained using the control techniques presented in the preceding section.

A. ANN model

Among many techniques used to construct approximations of the nonlinear behavior observed experimentally in electrochemical systems, the artificial neural networks have been one of the most successful ones [14]. Here, we employ one of the simplest and most widely used ANN configurations, a four-layer feedforward architecture [15], in order to construct a NMM map representation of the system that would serve as the basis to tune the feedback controller and apply the feedback-feedforward controller described in the preceding section. A similar ANN-model-based controller strategy has been previously exploited by Otawara and Fan [16] to stabilize periodic orbits in the presence of chaotic motion.

The ANN has a standard feedforward architecture with two 12-neuron hidden layers with sigmoidal activation. Inputs and outputs are assigned according to the form of the NMM model that one wishes to approximate [Eq. (4)]. The ANN was trained with data obtained via simulation of the original set of ordinary differential equations (ODEs)—Eqs. (1)–(3)—that represent the system that serves as the basis of the illustration described here. In an effort to make the simulations more realistic, we utilized only two sets of initial conditions:

$$Y=0.105, \quad \theta_{OH}=0.320, \quad \theta_O=0.1168, \tag{8a}$$

$$Y=0.114170, \quad \theta_{OH}=0.264339, \quad \theta_O=0.116420. \tag{8b}$$

TABLE I. ANN training data indicating parameter value at which the data were gathered, type of behavior observed, and numbers of points from each of the two initial points.

Parameter value	Behavior type	Points from (8a)	Points from (8b)
9.62×10^{-5}	Period 1	12	12
9.65×10^{-5}	Period 2	16	19
9.67×10^{-5}	Period 4	21	100
9.6865×10^{-5}	Period 6	21	27
9.7030×10^{-5}	Chaos	100	0
9.7195×10^{-5}	Chaos	100	0
9.7360×10^{-5}	Chaos	100	0
9.7525×10^{-5}	Chaos	100	0
9.7690×10^{-5}	Period 6	31	0
9.7855×10^{-5}	Period 3	15	29
9.8020×10^{-5}	Period 3	15	21
9.8185×10^{-5}	Period 3	15	0
9.8350×10^{-5}	Period 3	15	0
9.8515×10^{-5}	Period 3	19	20
9.8680×10^{-5}	Period 3	14	0
9.8845×10^{-5}	Period 8	33	41
9.9×10^{-5}	Period 2	10	41
10×10^{-5}	Period 2	13	14
10.1×10^{-5}	Period 3	20	0
10.2×10^{-5}	Period 1	15	12
Totals		685	336

The data was gathered at irregular parameter intervals in the range between $s=9.62\times10^{-5}$ and $s=10.2\times10^{-5}$. The transients trajectories (in a NMM map format) from the initial points were also included in the training data. In some cases (for chaotic behavior) only data from one of the two initial points was used. Table I summarizes the data used for the training, indicating the parameter value, the type of long-term behavior observed and the number of data points used for each of the two initial conditions. The training set was composed of a total of 1021 points.

The ANN was trained using the well-known backpropagation rules. The ANN parameters were randomly assigned at the start of the training in the range $[-0.2,+0.2]$. The training was performed using a conjugate gradient (CG) algorithm. Convergence was declared after 41 CG cycles using cross-validation techniques and a test set (data not included in the training set). The average error was below 1.2% of the active range of the variables in the training set. Table II shows the parameter values at which the test data were collected and it also compares the type of long-term behavior predicted with the observed type for the original set of ODEs.

The ANN model should be capable, as a minimum requirement, of reproducing the location and stability of the period-3 attractor over the entire parameter window of interest. This minimum requirement is fulfilled by the ANN constructed as can be appreciated in Fig. 1 in which we present the original and predicted behavior in the form of bifurcation diagrams of the NMM map. These bifurcation diagrams only

TABLE II. Parameter values and types of behavior for the test data used to declare convergence of the ANN training.

Parameter value	Original behavior	Predicted behavior
9.66×10^{-5}	Period 2	Period 2
9.685×10^{-5}	Period 3	Chaos
9.72×10^{-5}	Chaos	Chaos
9.84×10^{-5}	Period 3	Period 3
9.95×10^{-5}	Period 2	Period 2

present the long term behavior observed for each parameter value (transients are not included).

With the ANN model, we estimated the deviations in the prediction of the period-3 attractors. Figure 2 compares the location of the three points that constitute this attractor for the parameter values included in the training set. In general, the prediction is fairly good, except for a couple of points.

From Figs. 1 and 2 one can conclude that the ANN is an acceptable reference model for our system. It can predict reasonably the location of the period-3 solutions. We will use this model to tune the control parameters (proportional gains and radius of the *control region*) as well as the basis for the feedback-feedforward strategy.

It needs to be mentioned that the construction of the ANN model is independent of the model specifics making it in general applicable to other model systems and experimental situations.

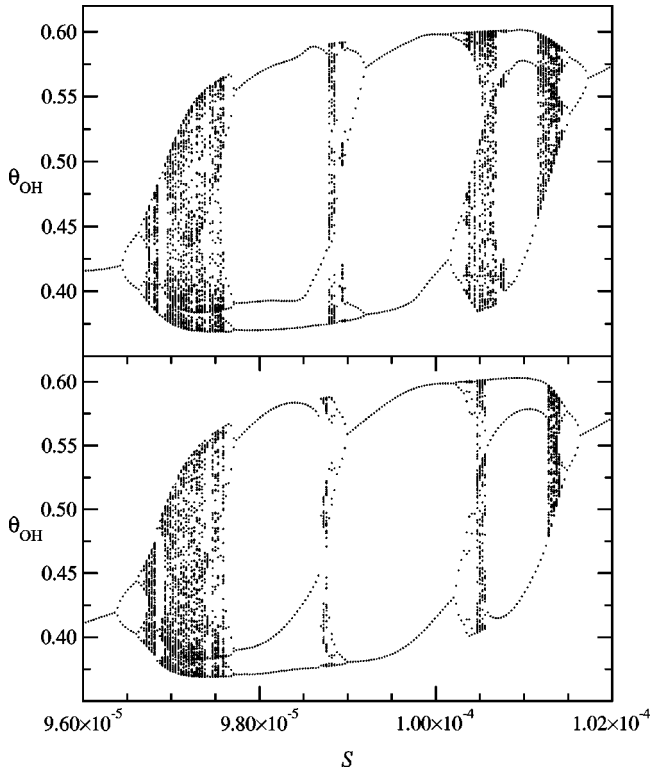

FIG. 1. Bifurcation diagram for the original system (top) and the ANN model (bottom). Besides the parameter s values noted in the figure, the remaining parameters of the original model were set as follows: $p=2\times10^{-4}$, $q=1\times10^{-3}$, $r=2\times10^{-5}$, and $\beta=5.0$.

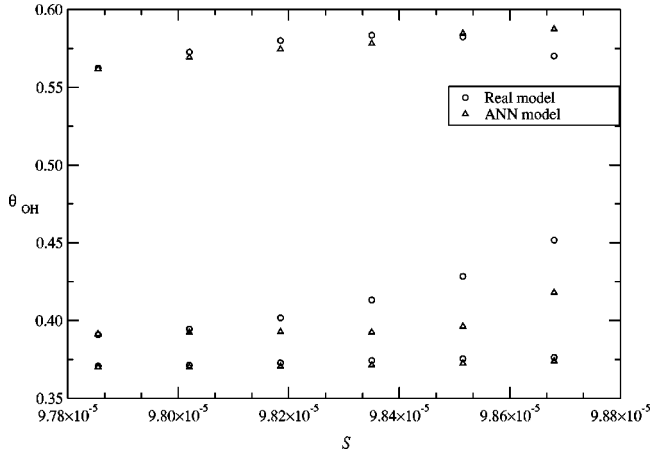

FIG. 2. Comparison of the predictions of the period-3 attractor in the parameter range of interest.

B. Proportional feedback control

The proportional feedback control seeks to apply a perturbation to the system parameter s whenever the dynamics drive the system to the *control region* (in the NMM representation). Once the system leaves the *control region*, the parameter is returned to its nominal operation value s_0.

As an illustration of its application we seek to destabilize the period-3 attractor observed at $s_0=9.8\times10^{-5}$. The ANN model is used to predict the location of the period-3 points under the NMM representation of the dynamics of the system. In this case, the ANN predicts the attractor as located in the following points:

$$0.568\,543\,1, \quad 0.370\,137\,2,$$

$$0.370\,137\,2, \quad 0.392\,326\,5,$$

$$0.392\,326\,5, \quad 0.568\,543\,1.$$

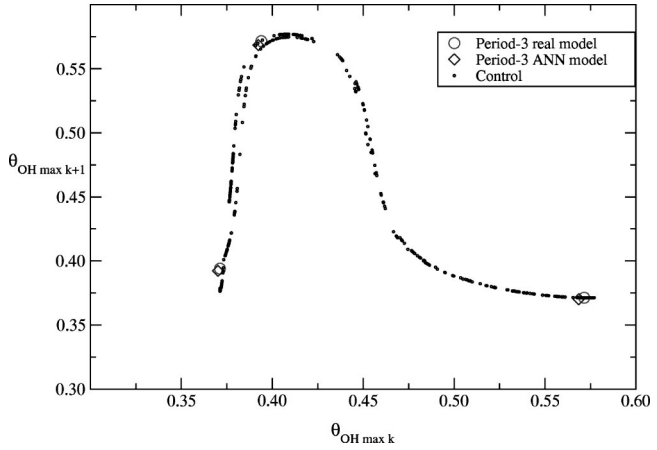

FIG. 3. Next-maximum-map representation of the trajectory of the system under the feedback control for $s_0=9.8\times10^{-5}$, $r_c=0.02$, and $\alpha=-0.005$. In the figure, the real period-3 attractor is represented by empty circles, the predicted period-3 attractor by diamonds, and the trajectory of the system by the filled small circles.

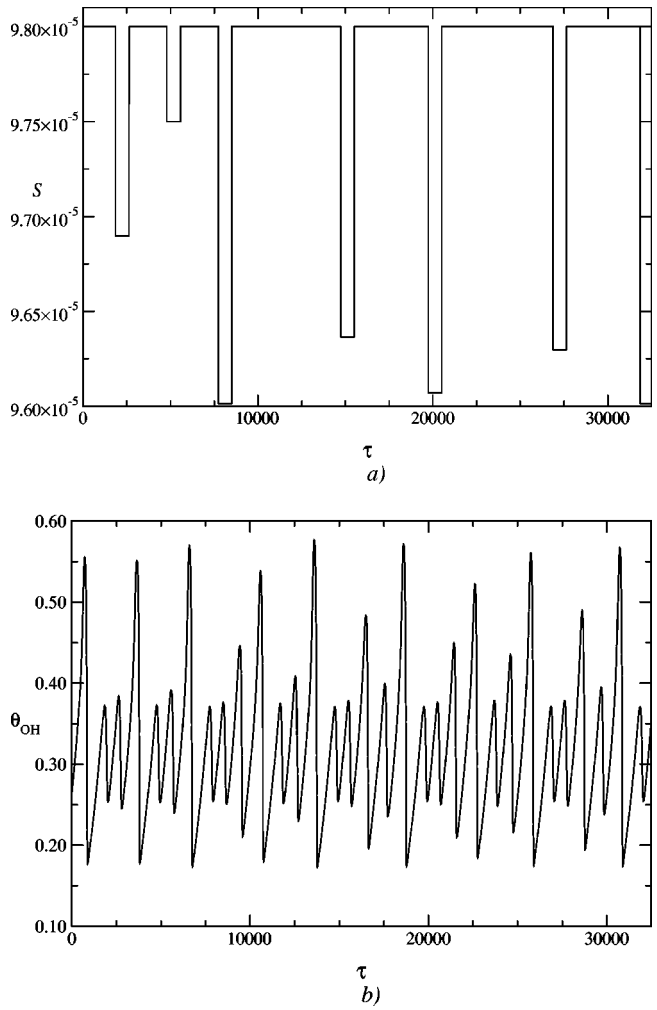

FIG. 4. (a) Parameter perturbations and (b) time series with $s_0 = 9.8\times10^{-5}$, $r_c = 0.02$, and $\alpha = -0.005$, for the system under the feedback control.

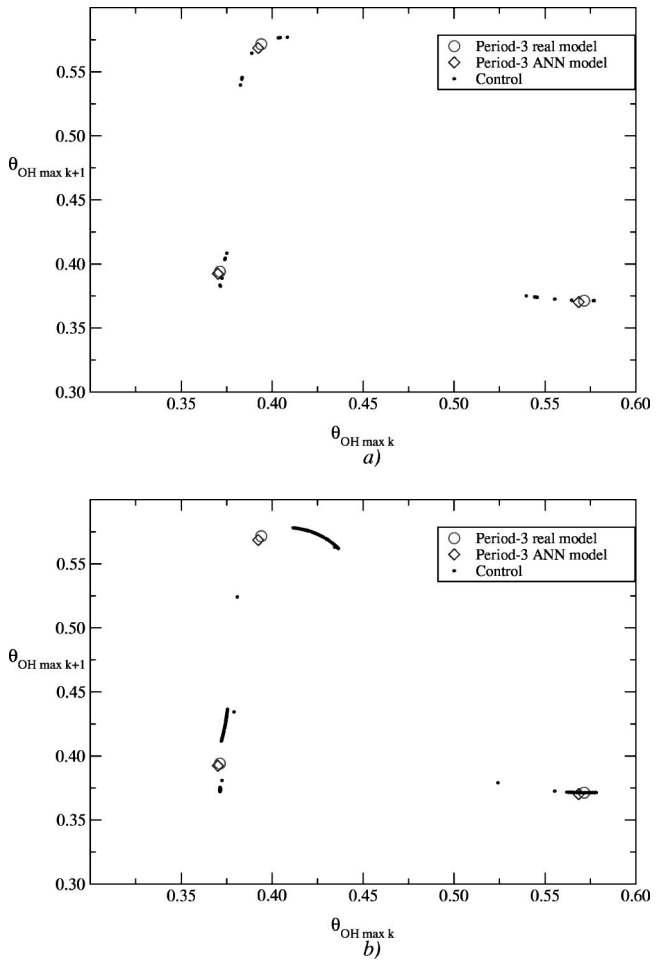

FIG. 5. Effect of the controller's proportional gain. (a) $\alpha = -0.003$ and (b) $\alpha = -0.007$; in both cases $s_0 = 9.8\times10^{-5}$ and $r_c = 0.02$.

From these points, we selected the first one (0.568 543 1,0.370 137 2) as the center of the *control region*. Any one of the points could be selected. Similar results are obtained for the other points as the center of the *control region*. One should also select the radius of the *control region*. This value is somewhat arbitrary, but it should be relatively small (in comparison with the active range of variations of the maxima in the time series of the variable θ_{OH}). In this case we select a value of $r_c = 0.02$, which is approximately 4% of the active range of the maxima for the variable θ_{OH}.

The value of the proportional gain α was found via simulations using the ANN model. Figure 3 exhibits an example of the chaotic-like behavior found using the feedback control with $\alpha = -0.005$. The sign of the gain indicates the direction of the perturbation. The system is perturbed towards lower values of s because the chaotic windows observed for such values are larger and thus the system achieves more easily the chaotic-like behavior.

The size of the perturbations applied to the parameter s are shown in Fig. 4(a). One can observe that the perturbations are applied for a short time interval before returning the parameter to its original setting. The largest parameter change applied is approximately of 2.0×10^{-6} units of s. Figure 4(b) shows the time series of the system that exhibits stabilization of the system dynamics on otherwise short-lived chaotic transients. The magnitude of the proportional gain is very important in determining the performance of the controller. Together with the radius of the *control region* r_c, the proportional gain determines the size of the perturbation applied to the parameter. Figure 5 illustrates the effect of this parameter over the performance of the controller for the same conditions as for Fig. 3. For Fig. 5(a) one observes a periodic attractor, while for Fig. 5(b), the attractor resembles a piecewise chaotic motion. Note that α for this figure was varied above and below the value used for Fig. 3 indicating that there exists a narrow range of values that one could use to enhance the chaotic motion. The ANN reference model was used to find this range of values (''tune'' the controller). Such strategy would find relevance in implementing this type of controllers to real experiments, one could easily bracket the range of values of the proportional gain appropriate to achieve the desired control of systems behavior.

For $\alpha = -0.003$, Fig. 5(a), the applied perturbation is not enough to drive the system to the chaotic window. Instead, it

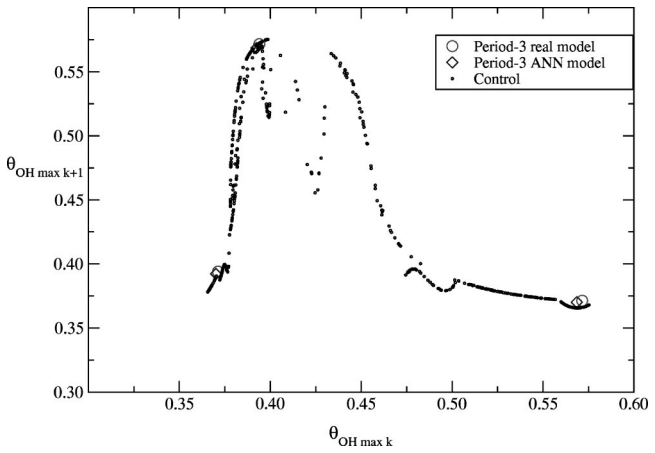

FIG. 6. NMM trajectory illustrating the application of the feedback-feedforward controller with $s=9.8\times10^{-5}$, $r_c=0.01$, $\alpha=-0.01$, and $\gamma=-0.005$.

appears that the system is driven towards another period-3 attractor. Since this new period-3 attractor falls outside the *control region*, no further perturbations are applied and the system does not follow a chaotic motion. For $\alpha=-0.007$, Fig. 5(b), the perturbation is very large and the systems appears to be driven towards the middle of the sequence of period-doubling bifurcations that gives rise to the chaotic motion. In this manner, the trajectory is moved towards what appears a piecewise chaotic attractor or a very high period orbit.

C. Feedback-feedforward control

Results from Secs. III A and III B indicate that the proportional feedback control succeeds in driving the system towards a chaotic-like motion; however, it requires an accurate prediction of the period-3 attractor location, or to resort to enlarging the *control region*. In order to refine the chaos anticontrol/enhancement with smaller control regions, and effectively prevent the system to reach the vicinity of the period-3 attractor, it seems necessary to resort to a different strategy. We propose the use of a feedback-feedforward controller that takes full advantage of the availability of a predictive reference model in the form of an ANN approximator. The ANN is used to predict when the trajectory will reach the *control region* and to apply an action to prevent this from happening. With this type of controller, the radius of the *control region* can be smaller than for the feedback-alone controller. Figure 6 illustrates the application of this controller with $r_c=0.01$ for the same conditions used for Fig. 3.

With the feedback-feedforward, even though the proportional gain is twice as large as for the feedback controller, one observes that the perturbations applied to the parameter are smaller, albeit more frequent. Figure 7 shows the parameter and time series resulting from applying this strategy for the conditions of Fig. 6. The maximum perturbation applied to the parameter is approximately 1.0×10^{-6}, about half as large as the perturbations needed for the feedback-alone controller. This controller with the correction term almost

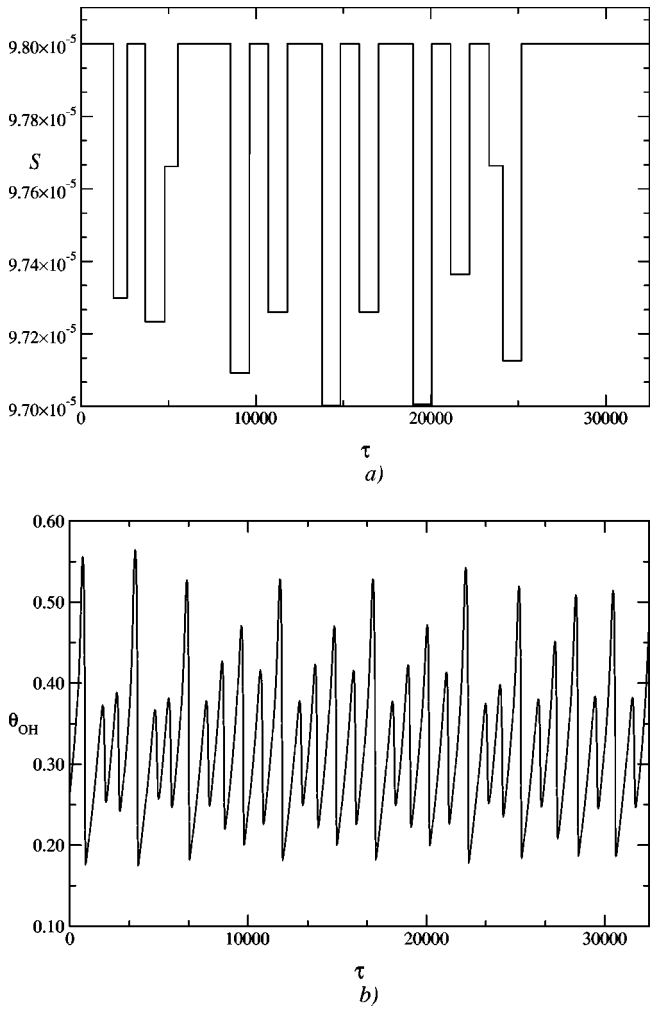

FIG. 7. (a) Parameter perturbation history s and (b) time series for the system under feedback-feedforward control with $s_0=9.8\times10^{-5}$, $r_c=0.01$, $\alpha=-0.01$, and $\gamma=-0.005$.

achieves a complete exclusion of the trajectories from the *control region*.

IV. CONCLUSIONS

Our main goal was to devise control strategies to enhance the chaotic motion for parameter windows for which one would normally observe a period-3 stable attractor. We propose two different strategies: one relying in feedback control alone and a second that takes advantage of the availability of a predictive reference model in the form of an artificial-neural-network approximator. The implementation of both strategies is illustrated using a realistic model for electrochemical corrosion and relying on the next-maximum-map representation for the evolution of the system trajectories. The control action applied in both cases is proportional to the distance of the current point to one of the points that define the period-3 attractor. The ANN reference model is used to estimate such location, tune the controller parameters, and provide a preventive correction for the case of the feedback-feedforward strategy. The feedback strategy is easily implemented, and utilizes only two parameters: the radius of the

control region and the gain of the proportional feedback action. Both parameters are straightforwardly tuned. However, the ''corrective'' nature of the feedback action could translate to an inefficient exclusion of the trajectories from the *control region*. The feedback-feedforward strategy, on the other hand, requires the availability of an accurate reference model and involves an additional controller parameter (proportional gain associated with the predictive term). Although some of the simplicity of the controller implementation is lost, this strategy results in a cleaner exclusion of the trajectories from the *control region* and more significantly requires smaller perturbations to maintain transient chaos.

ACKNOWLEDGMENT

The authors acknowledge continuous support from the Mexican Ministry of Public Education (CONACyT and CoSNET).

[1] E. Ott, C. Grebogi, and J. A. Yorke, Phys. Rev. Lett. **64**, 1196 (1990).
[2] W. L. Ditto, S. N. Rauseo, and M. L. Spano, Phys. Rev. Lett. **65**, 3211 (1990).
[3] E. R. Hunt, Phys. Rev. Lett. **67**, 1953 (1991).
[4] V. Petrov, V. Gáspár, J. Masere, and K. Showalter, Nature (London) **361**, 240 (1993).
[5] P. Parmananda, P. Sherard, R. W. Rollins, and H. D. Dewald, Phys. Rev. E **47**, R3003 (1993).
[6] A. Garfinkel, M. L. Spano, W. L. Ditto, and J. N. Weiss, Science **257**, 1230 (1992).
[7] S. J. Schiff, K. Jerger, D. H. Duong, T. Chang, M. L. Spano, and W. L. Ditto, Nature (London) **361**, 240 (1994).
[8] A. L. Goldberger, Ann. Biomed. Eng. **18**, 195 (1990).
[9] J. M. Ottino, Sci. Am. **260**, 40 (1989).
[10] W. Yang, M. Ding, A. Mandell, E. Ott, Phys. Rev. E **51**, 102 (1995).
[11] V. In, S. E. Mahan, W. L. Ditto, and M. L. Spano, Phys. Rev. Lett. **74**, 4420 (1995).
[12] J. B. Talbot and R. A. Oriani, Electrochim. Acta **30**, 1277 (1985).
[13] J. K. McCoy, P. Parmananda, R. W. Rollins, and A. J. Markworth, J. Mater. Res. **8**, 1858 (1993).
[14] R. Rico-Martínez, K. Krischer, M. C. Kube, I. G. Kevrekidis, and J. L. Hudson, Chem. Eng. Commun. **118**, 25 (1992).
[15] A. S. Lapedes and R. M. Farber, Los Alamos Report No. LA-UR-87-2662, 1987 (unpublished).
[16] K. Otawara and L. T. Fan, Proc. IEEE Int. Conf. **4**, 1943 (1995).